

Informative Path Planning and Mapping for Active Sensing under Localization Uncertainty

Marija Popović, Teresa Vidal-Calleja, Jen Jen Chung, Juan Nieto, Roland Siegwart

Abstract—Robotic platforms are emerging as a timely and cost-efficient tool for exploration and monitoring. However, an open challenge is planning missions for robust, efficient data acquisition in complex environments. To address this issue, we introduce an informative planning framework for active sensing scenarios that accounts for the robot pose uncertainty. Our strategy exploits a Gaussian Process model to capture a target environmental field given the uncertainty on its inputs. This allows us to maintain robust maps, which are used for planning information-rich trajectories in continuous space. A key aspect of our method is a new utility function that couples the localization and field mapping objectives, enabling us to trade-off exploration against exploitation in a principled way. Extensive simulations show that our approach outperforms existing strategies, with reductions of up to 45.1% and 6.3% in mean pose uncertainty and map error. We demonstrate a proof of concept in an indoor temperature mapping scenario.

I. INTRODUCTION

Rapid technological advancements are inciting the use of autonomous mobile robots for exploration and data acquisition. In many marine [1, 2], terrestrial [3, 4], and airborne [5, 6] applications, these systems have the ability to bridge the spatiotemporal divides limiting traditional measurement methods in a safer and more cost-effective manner [7]. However, to fully exploit their potential, algorithms are required for planning efficient informative paths in complex environments under platform-specific constraints.

This paper examines the problem of active sensing using a robot, where the aim is to map a 2-D or 3-D field, e.g., of temperature, humidity, etc., in a certain environment using measurements collected by an on-board sensor. Our motivation is to create robust, high-quality maps of the field by allowing the robot to adaptively trade-off between gathering new information and maintaining good localization. In similar set-ups, most existing strategies [1, 5, 8] assume perfect pose information, which is an implicit requirement for accurately reconstructing the target field. Despite recent efforts [2, 6, 9, 10], propagating both the localization and field map uncertainties into the planning framework in a principled manner remains a key challenge.

To address this, we present a new informative planning approach that explicitly accounts for the robot pose uncertainty in active sensing scenarios. We use Gaussian Processes (GPs) with uncertain inputs (UIs) [2] to propagate the pose estimation uncertainty into our environmental field model.

M. Popović, J. J. Chung, J. Nieto, and R. Siegwart are with the Autonomous Systems Lab., ETH Zürich, Zürich, Switzerland. T. Vidal-Calleja is with the Centre for Autonomous Systems at the Faculty of Engineering and IT, University of Technology Sydney, Australia. Corresponding author: mpopovic@ethz.ch.

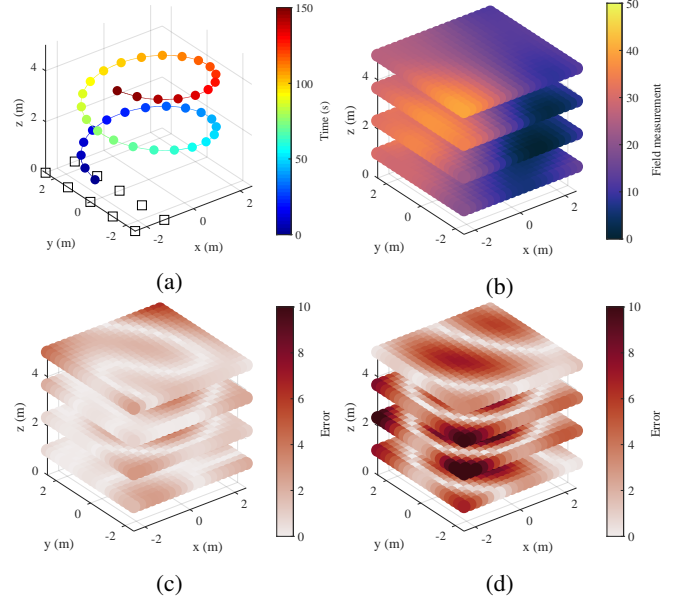


Fig. 1: Overview of our proposed active sensing strategy. (a) shows a spiral trajectory traveled by a robot. The squares indicate point landmarks on the ground used for localization. The spheres represent sites where measurements of the ground truth field map in (b) are taken. By accounting for pose estimation uncertainty, our framework yields an error map (c) with 2.47 times lower cumulative error compared to a standard mapping approach (d).

During a mission, the map built online is used to plan informative trajectories in continuous space by optimizing initial solutions obtained by a coarse grid search. We introduce a utility function that jointly considers the uncertainty of the robot and the field map, thereby enabling us to trade off between exploitation and exploration in a mathematically sound manner. The contributions of this work are:

- 1) A utility function for general active sensing problems that tightly couples the objectives of robot localization and field mapping.
- 2) Its integration in an informative planning framework with probabilistic localization-based back end systems and the evaluation of our approach in a graph simultaneous localization and mapping (SLAM) set-up.
- 3) Proof of concept through autonomously executed tests.

We note that our framework can be used in any scalar field mapping scenario, e.g., spatial occupancy [4, 6, 11], signal strength [2, 8], aerial surveillance [5, 7], etc., and with any SLAM or localization-only back end. Moreover, the applicability of our utility function extends to other areas of robotics, such as reinforcement learning [12].

II. RELATED WORK

Significant recent work has been done on autonomous information gathering problems. The discussion in this section focuses on two main research streams: methods of environmental modeling [2, 6, 9, 13] and planning algorithms for efficient data acquisition [1, 4, 5, 11, 14, 15].

GPs are a popular non-parametric Bayesian technique for modeling spatio-temporal phenomena [13]. They have been applied in various active sensing scenarios [1, 3, 5, 15] to gather data based on correlations and uncertainty in continuous maps. However, most of these works assume that the training data for prediction is inherently noise-free, which may lead to inaccuracies and mislead planning algorithms.

Propagating the input uncertainty through dense GP models is a computationally challenging task. To address this, analytical [9] and heteroscedastic approximation methods [2, 3, 10] have been proposed. Our work leverages the expected kernel approach of Jadidi et al. [2] by integrating over UIs with deterministic query points. We extend this approach to 3-D scenarios, enabling us to generate robust maps under robot pose uncertainty for online planning applications.

The active sensing task can be expressed in a partially observable Markov decision process (POMDP) [16] as one of decision-making under uncertainty. In practice, informative planning algorithms are typically used to render this problem computationally tractable with dense belief representations. We broadly distinguish between (i) discrete [4, 11] and (ii) continuous strategies. This study focuses on the latter class of methods, which leverage incremental sampling [6, 8, 17, 18] or splines [1, 5] to offer greater scalability. As in our prior work [5, 14, 15], we define smooth polynomial robot trajectories [19] and optimize them globally for an informative objective in a finite-horizon manner.

Relatively limited research has been invested in planning scenarios where robot localization is uncertain. This set-up has been tackled in the contexts of belief-space planning [6, 17, 18] and active SLAM [11, 20], where the aim is to maintain good localization as an unknown environment is explored. Similarly to Papachristos et al. [6] and Costante et al. [17], our paper considers a setting where the map building and localization problems are decoupled. In contrast, however, we aim to reconstruct a continuous field in the environment which is independent of its geometry.

A key challenge in this set-up is trading off between robot localization and field mapping in a principled manner. To address this, previous approaches have examined heuristic tuning [11, 20] and two-step [6, 17] planning strategies. Our method follows Carrillo et al. [4] in using Rényi's entropy to discount information gain based on predicted localization uncertainty, which allows us to couple the two objectives in a mathematically sound way. The core difference is that we adapt these concepts to a continuous mapping scenario using a GP field model with UIs. Thereby, we present a general unified framework where robot localization uncertainty is jointly accounted for in both mapping and planning.

III. PROBLEM STATEMENT

The active sensing problem is formulated as follows. We seek an optimal trajectory ψ^* in the space of all continuous trajectories Ψ to maximize an information-theoretic measure:

$$\begin{aligned} \psi^* &= \operatorname{argmax}_{\psi \in \Psi} \mathbb{I}[\text{MEASURE}(\psi)], \\ &\text{s.t. } \text{COST}(\psi) \leq B. \end{aligned} \quad (1)$$

The function $\text{MEASURE}(\cdot)$ obtains a finite set of measurements along trajectory ψ and $\text{COST}(\cdot)$ provides its associated cost, which cannot exceed a predefined budget B . The operator $\mathbb{I}[\cdot]$ defines the informative objective quantifying the utility of the acquired measurements. In [Section V-C](#), we propose a utility function for active sensing which incorporates both robot localization and field mapping objectives.

IV. MAPPING APPROACH

This section presents our mapping approach as the basis of our framework. We first describe our method of environmental field modeling using a GP, then present a strategy which folds the robot pose uncertainty into the map inference.

A. Gaussian Processes

We use a GP to model spatial correlations in a probabilistic and non-parametric manner [13]. The target field variable for mapping is assumed to be a continuous function: $f : \mathcal{E} \rightarrow \mathbb{R}$. A Gaussian correlated prior is placed over the function space, which is fully characterized by the mean function $m(\mathbf{x}) = \mathbb{E}[f(\mathbf{x})]$ and covariance function $k(\mathbf{x}, \mathbf{x}') = \mathbb{E}[(f(\mathbf{x}) - m(\mathbf{x}))(f(\mathbf{x}') - m(\mathbf{x}'))]$ as $f(\mathbf{x}) \sim \mathcal{GP}(m(\mathbf{x}), k(\mathbf{x}, \mathbf{x}'))$, where $\mathbb{E}[\cdot]$ is the expectation operator.

Let $\mathbf{x}_i \subset \mathcal{E}$ be a set of n observed input training points in the fixed-size environment with associated target values y_i . For a set of n^* query points $\mathbf{x}_i^* \subset \mathcal{E}$, we can evaluate the predictive conditional Gaussian distribution $f(X^*) \sim \mathcal{N}(\bar{f}^*, \text{cov}(f^*))$ as follows [13]:

$$\begin{aligned} \bar{f}^* &= m(X^*) + K(X^*, X)[K(X, X) + \sigma_n^2 I]^{-1} \times \\ &\quad (y - m(X)), \\ \text{cov}(f^*) &= K(X^*, X^*) - K(X^*, X)[K(X, X) + \sigma_n^2 I]^{-1} \times \\ &\quad K(X^*, X)^\top, \end{aligned} \quad (2)$$

where σ_n^2 is a hyperparameter representing observation noise variance, $K(X^*, X)$ denotes cross-correlation terms between the query and observed points, and $K(X, X)$ and $K(X^*, X^*)$ are the joint covariance matrices for the observed and query points, respectively. Note that $K(\cdot, \cdot)$ corresponds to $k(\cdot, \cdot)$ for only one element.

To describe environmental phenomena, we propose using a constant mean function $m(\mathbf{x}) = m_{gp}$ and the isotropic squared exponential (SE) kernel common in geostatistical analysis. It is defined as [13]:

$$k_{SE}(\mathbf{x}, \mathbf{x}^*) = \sigma_f^2 \exp\left(-\frac{d^2}{2l^2}\right), \quad (4)$$

where d is the Euclidean distance between inputs \mathbf{x} and \mathbf{x}^* , and l and σ_f^2 are hyperparameters representing the lengthscale and signal variance, respectively.

The resulting fixed hyperparameters $\theta = \{m_{gp}, \sigma_n^2, \sigma_f^2, l\}$ control relations within the GP. These values can be optimized by training data to match the properties of f by minimizing log marginal likelihood [13].

B. Mapping Under Pose Uncertainty

To propagate the robot pose uncertainty into our mapping framework, we extend the expected kernel technique of Jaidi et al. [2] to 3-D set-ups. The key idea lies in taking the expectation of the covariance function over UIs. Let $\mathbf{x} \in \mathcal{X}$ be a random variable distributed according to a probability distribution $p(\mathbf{x})$. The expected covariance function \tilde{k} can be computed as:

$$\tilde{k} = \mathbb{E}[k] = \int_{\mathcal{X}} k p(\mathbf{x}) d\mathbf{x}. \quad (5)$$

Assuming a Gaussian distribution for the robot pose $\mathcal{N}(\mathbf{p}, \Sigma)$, we apply Gauss-Hermite quadrature to efficiently approximate the integral in Equation (5) in three dimensions.

V. PLANNING APPROACH

This section overviews our planning scheme, which generates fixed-horizon plans through a combination of a 3-D grid search and evolutionary optimization. We summarize the key steps, focusing on our proposed uncertainty-aware utility function as the main contribution. For further details, the reader is referred to our previous works [5, 14, 15].

A. Trajectories

A polynomial trajectory ψ is represented by N ordered control waypoints to visit $\mathcal{C} = [\mathbf{c}_1, \dots, \mathbf{c}_N]$ connected using $N - 1$ k -order spline segments. Given a reference velocity and acceleration, we optimize the trajectory for smooth minimum-snap dynamics [19], clamping \mathbf{c}_1 as the initial robot position. In Equation (1), MEASURE(\cdot) is defined by computing the spacing of measurement sites given a constant sensor frequency and the traveling speed of the robot.

B. Algorithm

We plan adaptively using a fixed-horizon approach, alternating between replanning and execution until the elapsed time t exceeds the budget B . Our replanning strategy (Algorithm 1) consists of two steps. First, an initial trajectory is obtained through a coarse grid search (Lines 3-7) based on a lattice \mathcal{L} in the robot workspace. In this step, we conduct a sequential greedy search for N control waypoints in \mathcal{C} ; selecting the next-best point \mathbf{c}^* (Line 4) by evaluating Equation (1) over \mathcal{L} with the proposed utility function in Equation (8). For each goal \mathbf{c}^* , the evolution of the robot pose uncertainty Σ during travel is predicted using the SLAM back end (Line 5), as detailed in Section V-D. The result is then used to update the field model \mathcal{GP} (Line 6) and is added to the initial trajectory solution (Line 7).

The grid search allows for quickly obtaining a rough solution for \mathcal{C} , which is then refined to maximize the informative objective. In this step (Line 8), we employ the Covariance Matrix Adaptation Evolution Strategy (CMA-ES) [21], a generic evolutionary optimization routine, to

solve Equation (8) for a sequence of measurements along the trajectory.

Algorithm 1 REPLAN_PATH procedure

Input: Current environment model \mathcal{GP} , number of control waypoints N , lattice points \mathcal{L} , robot pose (\mathbf{p}, Σ)

Output: Waypoints defining next polynomial plan \mathcal{C}

- 1: $\mathcal{GP}' \leftarrow \mathcal{GP}$; $(\mathbf{p}', \Sigma') \leftarrow (\mathbf{p}, \Sigma)$ // Create local copies.
 - 2: $\mathcal{C} \leftarrow \emptyset$ // Initialize control points.
 - 3: **while** $N \geq |\mathcal{C}|$ **do**
 - 4: $\mathbf{c}^* \leftarrow$ Select viewpoint in \mathcal{L} using Equation (1)
 - 5: $(\mathbf{p}', \Sigma') \leftarrow$ PREDICT_MOTION(\mathbf{p}' , Σ' , \mathbf{c}^*)
 - 6: $\mathcal{GP}' \leftarrow$ PREDICT_MEASUREMENT(\mathcal{GP}' , \mathbf{p}' , Σ')
 - 7: $\mathcal{C} \leftarrow \mathcal{C} \cup \mathbf{c}^*$
 - 8: $\mathcal{C} \leftarrow$ CMAES(\mathcal{C} , \mathcal{GP} , \mathbf{p} , Σ) // Optimize polynomial trajectory.
-

C. Utility Definition

We propose a new utility, or information gain, function $I[\cdot]$ in Equation (1) which considers the uncertainty of both the robot and the field map in a unified manner without any heuristic tuning. The key idea is to enable the robot to trade off between gathering new information and maintaining good localization to achieve more conservative mapping behavior.

Our utility function discounts the information value by the robot localization uncertainty following an approach similar to that of Carrillo et al. [4]. To quantify information in our field model, we leverage the definition of Rényi's entropy for a distribution $Y \sim \mathcal{N}(\mu, \sigma^2)$, given by [22]:

$$H_\alpha[Y] = \frac{1}{2} \log 2\pi\sigma^2 \alpha^{\frac{1}{\alpha-1}}, \quad (6)$$

where $\alpha \in [0, 1) \cup (1, \infty)$ is a free parameter, restricted in this work to the range $(1, \infty)$. Note that $H_{\alpha \rightarrow 1}[Y] = H[Y]$ converges to Shannon's entropy in the limiting case.

Applying this concept our GP model with n observed training points X , we drop the constant terms above to obtain:

$$\hat{H}_\alpha[X] \propto \log \text{Tr}(\text{cov}(f^*)) \alpha^{\frac{1}{\alpha-1}}, \quad (7)$$

where $\text{cov}(f^*)$ is obtained using Equation (4) or Equation (5) for mapping without or with UIs, respectively.

We relate α to the pose uncertainty Σ predicted after the robot moves to a point \mathbf{p} , such that poorer localization decreases the expected information gain. Specifically, this study considers a simple relationship with the A-optimal uncertainty criterion as $\alpha(\Sigma) = 1 + \frac{1}{\text{Tr}(\Sigma)}$ [4], where $\text{Tr}(\cdot)$ denotes the matrix trace.

To measure the information gain associated with \mathbf{p} , we compute the mutual information between the training data of the current GP field model X and the new sensor observations acquired Z . Our utility function is defined as:

$$I[X; Z] = \hat{H}[X] - \hat{H}_{\alpha(\Sigma)}[X|Z]. \quad (8)$$

Our main insight is to scale the expected GP model entropy $\hat{H}_{\alpha(\Sigma)}[X|Z]$ by the pose uncertainty at \mathbf{p} via the Rényi parameter $\alpha(\Sigma)$. This achieves the trade-off between localization and field mapping in a meaningful way.

D. Uncertainty Prediction

A key ingredient of our planning algorithm is propagating the robot localization uncertainty for a candidate action (Line 5 of [Algorithm 1](#)). In unknown environments, we propose a solution to this problem assuming a graph-based SLAM back end using odometry and 3-D point landmark observations as constraints [23]. To predict the localization uncertainty along a candidate trajectory, the graph is simply extended from the current pose. The trajectory is interpolated with a fixed frequency to add odometry constraints in the extended graph. For each consecutive node pair, we apply control noise drawn from a Gaussian distribution whose variance is proportional to the control input magnitude. This caters for the fact that longer motion steps are likely to have higher actuation errors associated with them.

To address potential loop closures, we simulate re-observations to the known landmarks maintained in the current graph. In unknown space, we assume that no new landmarks will be detected, causing the robot pose uncertainty to grow. The resulting graph is then solved using QR factorization. Future work will extend these ideas to alternative SLAM systems and consider sparsification methods [24] for real-time application in larger areas.

Similarly, in a known environment, uncertainty prediction can be achieved using a motion model and the expected sensor measurements obtained assuming a Monte Carlo Localization (MCL) approach. In [Section VI-C](#), we apply this method to localize a robot equipped with a laser scanner in an indoor area.

VI. EXPERIMENTAL RESULTS

In this section, we validate our approach in simulation by comparing it to different strategies for planning and mapping. We then show proof of concept by using it to map temperature using a ground robot in an indoor environment.

A. Comparison of Planning Methods

To assess our proposed utility function, we first compare it to alternative planning methods using our GP-based mapping approach with UIs ([Section IV-B](#)). The evaluation is conducted in a simulated $5 \times 5 \times 4$ m Gaussian Random Field environment. For mapping, we use a $0.25 \times 0.25 \times 1$ m resolution grid and apply the SE kernel in [Equation \(4\)](#) with hyperparameters $\theta = \{m_{gp}, \sigma_n^2, \sigma_f^2, l\} = \{17.61, 2.13 \times 10^{-11}, 1141.38, 2.18\}$ trained by log-likelihood minimization [13]. Its modified variant in [Equation \(5\)](#) is estimated using Gauss-Hermite quadrature with 5 points. During a mission, field measurements are taken at 0.25 Hz using a point-based sensor centered on the robot. These are added to our GP model as observed input training points to achieve uncertainty reduction as exploration takes place.

To emulate an aerial robot set-up, 10 point landmarks are uniformly placed on the ground 1 m below the target field. For SLAM, the robot is equipped with a downward-facing camera with $(47.9^\circ, 36.9^\circ)$ field of view. Our framework uses a graph-based SLAM back end [23] with the uncertainty prediction approach in [Section V-D](#). We sample trajectories

at 0.5 Hz to simulate control actions, applying a coefficient of 0.01 in all three co-ordinate dimensions to scale the control noise variance. For planning, covariance matrices from the graph are extracted through the computations developed by Kaess and Dellaert [25].

Our Rényi-based utility function is compared against our framework using different objectives: (i) field map uncertainty reduction only ([Equation \(8\)](#) using standard Shannon’s entropy) and (ii) field map uncertainty reduction over time (rate), as in our previous works [5, 14, 15]. As benchmarks, we also study: (iii) the sampling-based rapidly exploring information gathering tree (RIG-tree) [8] and (iv) random waypoint selection. A 150 s budget is specified for all methods. To evaluate mapping performance, we quantify uncertainty with the GP covariance matrix trace and accuracy with Root Mean Squared Error (RMSE) with respect to the ground truth map. Similarly, for planning, our measures are the robot covariance matrix trace $\text{Tr}(\Sigma)$ and the robot pose error RMSE with respect to the ground truth trajectory. Intuitively, lower values for all metrics signify better performance.

The starting robot position is (2 m, 2 m, 1 m) with no prior information about the environment. For trajectory optimization, the reference velocity and acceleration are 1.5 m/s and 3 m/s^2 using polynomials of order $k = 12$. In our planner, we define polynomials with $N = 4$ waypoints and use a uniformly spaced 27-point lattice for the 3-D grid search. In RIG-tree, we associate control waypoints with vertices, and form polynomials by tracing the parents of leaf vertices to the root. The finite-horizon replanning procedure follows the approach of Popović et al. [5] with the uncertainty-only objective and a branch expansion step-size of 5 m empirically set for best performance based on multiple trials. In the random planner, random destinations are sampled in the environment and a trajectory is generated by connecting them sequentially to the current robot position. We consider 4 waypoints per plan to ensure that the trajectory lengths are fairly comparable to our method. [Figure 2](#) shows how the metrics evolve for each planner over 50 mission trials. As expected, the informed strategies perform better than the random benchmark (purple) as they are guided by mapping heuristics. The uncertainty-based utility functions (blue, red) yield map uncertainty and error reduction rates similar to our Rényi-based objective (yellow). However, our method significantly improves robot pose estimation in the same scenario. This confirms that it effectively trades off between gathering information and maintaining good localization by exploiting the known map. In this respect, the uncertainty-only function (blue) performs worst as it utilizes no knowledge of the trajectory dynamics.

Interestingly, RIG-tree (green) scores comparatively well on the localization metrics whereas the rate of map refinement is limited. This likely relates to the step-size parameter, which sets the range of navigation achievable during the mission. By traveling shorter trajectories, the robot re-observes landmarks more frequently at the cost of restricted exploration.

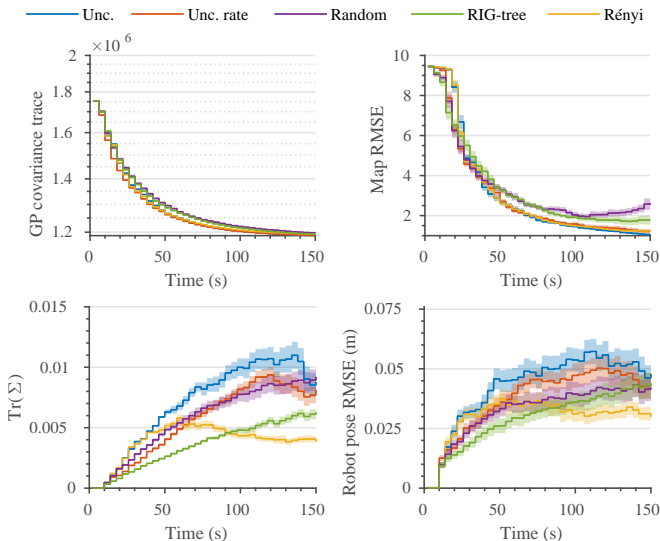


Fig. 2: Comparison of our Rényi-based utility function against planning benchmarks for a fixed budget of 150 s using GP mapping with UIs. The solid lines represent means over 50 trials. The shaded regions show 95% confidence bounds. By considering both the robot and field map uncertainties, our planner more quickly achieves higher-quality mapping (top) with improved localization (bottom). Note that the GP covariance trace is plotted on a logarithmic scale.

An example result using our Rényi-based utility function is shown in Figure 3. Figure 3a confirms that the robot successfully explores the environment, while re-visiting the known landmarks to maintain localization. With an RMSE of 1.11, the final map in this instance (Figure 3b) is 1.86 times more accurate than the one produced by the naïve spiral path in Figure 1, thus justifying our informative planning strategy.

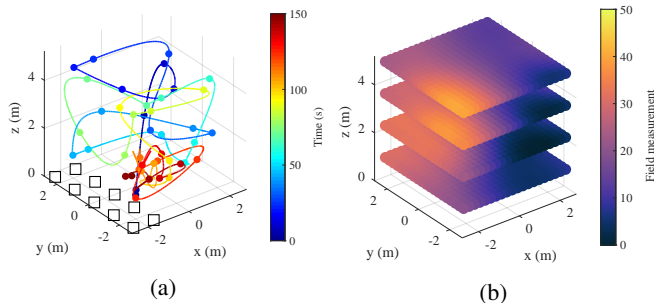


Fig. 3: Example result using our Rényi-based utility function. (a) shows the trajectory traveled by the robot. The squares indicate point landmarks used for localization. The spheres represent sites where measurements are taken to produce the final field map in (b). By balancing between gathering information and keeping the landmarks in view, our planner achieves 1.86 lower field map RMSE compared to the spiral path in Figure 1.

B. Evaluation of Field Mapping Under Uncertainty

Next, the effects of incorporating UIs in the GP field model are studied to evaluate mapping under the robot pose uncertainty. We consider the same simulation set-up as above using our proposed Rényi-based utility function

for planning. We conduct 50 trials each (i) with and (ii) without applying the modified kernel in Section IV-B. Note that (ii) corresponds to a standard GP mapping approach as a benchmark.

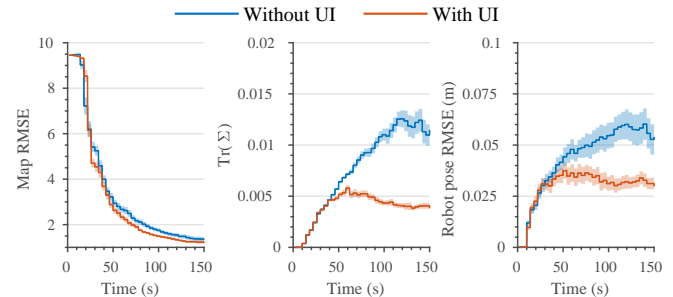


Fig. 4: Comparison of field mapping with and without uncertain inputs (UIs) using our Rényi-based utility function for a fixed budget of 150 s. The solid lines represent means over 50 trials. The shaded regions show 95% confidence bounds. By accounting for the robot pose uncertainty, our approach achieves more conservative mapping behavior (middle, right) with higher accuracy (left).

Our results are depicted in Figure 4. Note that we omit the map uncertainty metric as the variance scales using the two approaches are not comparable. The plots confirm that our approach with UIs (red) presents more conservative exploratory behavior than the benchmark (blue) while yielding more accurate maps. This is because our modified kernel can handle localization errors to improve the map quality, which is then coupled with the planning objective, as illustrated for an example trajectory in Figure 1.

C. Experiments

We show our active sensing framework running in real-time on a TurtleBot3 Waffle with an Intel Joule 570x running Ubuntu Linux 16.04 and the Robot Operating System. The experiments are conducted in a known indoor environment using Adaptive Monte Carlo Localization (AMCL) receiving data from a LDS-01 laser distance scanner. As shown in Figure 5b, for field mapping, a temperature distribution in an empty 2.8×2.8 m area within the environment is generated using a 2400 W radiant heater placed at one corner. Measurements are taken using a LM35 linear temperature sensor with a sensitivity of $10 \text{ mV}/^\circ\text{C}$.

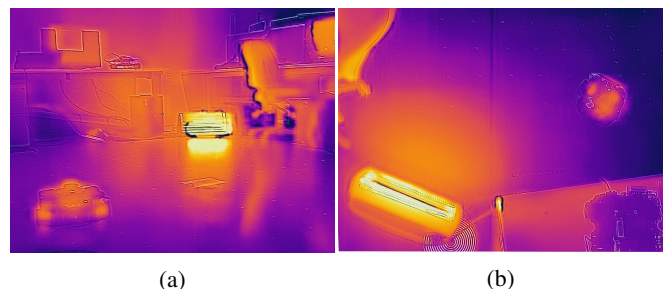


Fig. 5: Thermal imagery of our experimental set-up from side (a) and aerial (b) viewpoints. The robot and radiator are visible. Yellower shades correspond to heated areas mapped using measurements from the on-board temperature sensor.

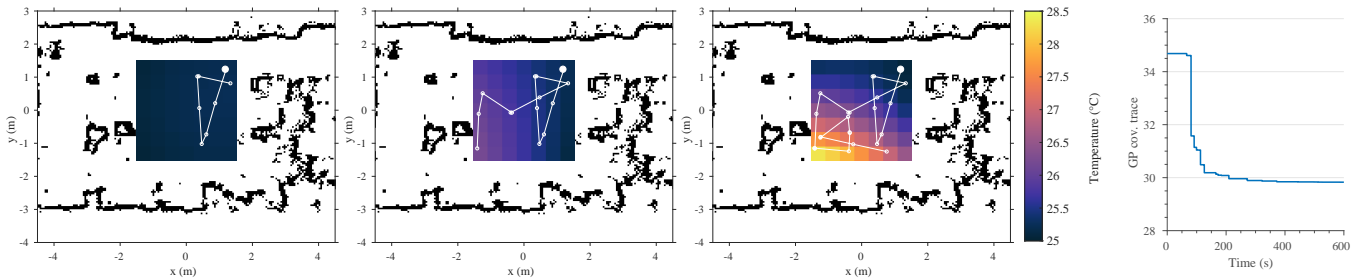


Fig. 6: Experimental results of using our active sensing framework to map the indoor temperature distribution in Figure 5 in a 600 s mission. The three plots on the left depict the trajectories (white lines) and temperature field maps (colored gradients) at different snapshots of the mission at times $t = 100$ s, 350 s, and 600 s. The white circles represent measurement sites, with the large solid one indicating the initial robot position. Yellower shades correspond to hotter regions. The sequence shows that our planner quickly explores the area, successfully detecting the heated corner (bottom-left) where the radiator is located. The curve on the right shows the uncertainty reduction in the field map over time, thus validating our approach. Note that planning time is taken into account.

A 0.4 m resolution grid is set for mapping with UIs. To train the GP model, we follow the method in Section VI-B using manually gathered data within the target area to obtain hyperparameters $\theta = \{m_{gp}, \sigma_n^2, \sigma_f^2, l\} = \{23.64, 3.6 \times 10^{-3}, 1.21, 5.23\}$ for the SE kernel. As before, the integral in Equation (5) is estimated using 5 Gauss Hermite points.

Our uncertainty prediction method is based on localization in a known environment using AMCL (Section V-D). We sub-sample each candidate plan at 2 Hz and estimate the robot pose using a differential drive odometry model and laser scans simulated in the known occupancy map. For the odometry model, variance parameters of 0.2 are used for Gaussian noise in both rotational and translational motion.

The aim is to show that our framework can map a realistic continuous field using a practical localization system. The initial measurement point is (0.2 m, 0.2 m) within the corner opposite the radiator. We allocate a planning budget B of 600 s. Following the differential drive model, each plan is piecewise linear as defined by $N = 3$ control waypoints with a constant velocity of 0.26 m/s and temperature measurements sampled at 0.25 Hz. The planning objective is our Rényi-based utility function in Equation (8). Note that the field map updates are triggered upon allowing the sensor readings to stabilize between measurement points.

Figure 6 summarizes our experiments. As expected, the field map becomes more complete over time and uncertainty decreases as the yellower heated region is discovered, thereby validating the applicability of our approach. Note that the mean value of the GP is lower than the range of measurements obtained due to the effects of heating and diffusion making it difficult to obtain a controlled temperature field. This motivates addressing temporal dynamics as a potential direction for future work.

VII. CONCLUSIONS AND FUTURE WORK

This work introduced an informative planning framework for active sensing problems that accounts for the robot pose uncertainty. Our method uses GPs with UIs to propagate the pose uncertainty into the model of a target environmental field. The resulting maps are used for informative planning by optimizing trajectories initialized by a course grid search.

A key aspect of our approach is a new utility function that tightly couples both robot localization and field mapping objectives. Specifically, we discount the information gain based on the predicted pose uncertainty to trade off between exploration and exploitation in a principled manner.

Our framework was evaluated extensively in simulation. We showed that it achieves more conservative exploratory behavior compared to different planning and mapping strategies, while producing more accurate maps. Proof of concept experiments validated the applicability of our approach in a temperature mapping scenario with real-time requirements.

Future work will examine field models with temporal dynamics and efficiency improvements to handle more complex environments. Other promising research directions involve refining the uncertainty prediction method and its relationship to the Rényi parameter for more reliable planning.

REFERENCES

- [1] G. Hitz, E. Galceran, M.-È. Garneau, F. Pomerleau, and R. Siegwart, "Adaptive Continuous-Space Informative Path Planning for Online Environmental Monitoring," *Journal of Field Robotics*, vol. 34, no. 8, pp. 1427–1449, 2017.
- [2] M. G. Jadidi, J. V. Miro, and G. Dissanayake, "Sampling-based Incremental Information Gathering with Applications to Robotic Exploration and Environmental Monitoring," 2016.
- [3] R. Oliveira, L. Ott, V. Guizilini, F. Ramos, and R. O. Sep, "Bayesian Optimisation for Safe Navigation under Localisation Uncertainty," in *International Symposium of Robotics Research*. Puerto Varas: Springer, 2017.
- [4] H. Carrillo, P. Dames, V. Kumar, and J. A. Castellanos, "Autonomous robotic exploration using a utility function based on Rényi's general theory of entropy," *Autonomous Robots*, vol. 42, no. 2, pp. 235–256, 2018.
- [5] M. Popović, T. Vidal-Calleja, G. Hitz, J. J. Chung, I. Sa, R. Siegwart, and J. Nieto, "An informative path planning framework for UAV-based terrain monitoring," *Autonomous Robots*, 2019, under review, arXiv preprint [arXiv:1809.03870](https://arxiv.org/abs/1809.03870).
- [6] C. Papachristos, S. Khattak, and K. Alexis, "Uncertainty-aware Receding Horizon Exploration and Mapping using Aerial Robots," in *IEEE International Conference on Robotics & Automation*. Singapore City: IEEE, 2017, pp. 4568–4575.
- [7] S. Manfreda, M. F. McCabe, P. E. Miller, R. Lucas, V. P. Madrigal, G. Mallinis, E. B. Dor, D. Helman, L. Estes, G. Ciraolo, J. Müllerová, F. Tauro, M. I. de Lima, J. L. de Lima, A. Maltese, F. Frances, K. Caylor, M. Kohv, M. Perks, G. Ruiz-Pérez, Z. Su, G. Vico, and B. Toth, "On the Use of Unmanned Aerial Systems for Environmental Monitoring," *Remote Sensing*, vol. 10, no. 4, 2018.
- [8] G. A. Hollinger and G. S. Sukhatme, "Sampling-based robotic in-

- formation gathering algorithms,” *International Journal of Robotics Research*, vol. 33, no. 9, pp. 1271–1287, 2014.
- [9] A. Girard, “Approximate methods for propagation of uncertainty with Gaussian process models,” Ph.D. dissertation, University of Glasgow, 2004.
- [10] A. Mchutchon and C. E. Rasmussen, “Gaussian Process Training with Input Noise,” *Advances in Neural Information Processing Systems*, pp. 1341–1349, 2011.
- [11] R. Valencia, J. V. Miró, G. Dissanayake, and J. Andrade-Cetto, “Active Pose SLAM,” in *IEEE/RSJ International Conference on Intelligent Robots and Systems*, Vilamoura, 2012, pp. 1885–1891.
- [12] S. D. Whitehead and D. H. Ballard, “Active Perception and Reinforcement Learning,” *Neural Computation*, vol. 2, no. 4, pp. 409–419, 2008.
- [13] C. E. Rasmussen and C. K. I. Williams, *Gaussian Processes for Machine Learning*. Cambridge, MA: MIT Press, 2006.
- [14] M. Popović, G. Hitz, J. Nieto, I. Sa, R. Siegwart, and E. Galceran, “Online Informative Path Planning for Active Classification Using UAVs,” in *IEEE International Conference on Robotics and Automation*. Singapore: IEEE, 2017.
- [15] M. Popović, T. Vidal-Calleja, G. Hitz, I. Sa, R. Y. Siegwart, and J. Nieto, “Multiresolution Mapping and Informative Path Planning for UAV-based Terrain Monitoring,” in *IEEE/RSJ International Conference on Intelligent Robots and Systems*. Vancouver: IEEE, 2017.
- [16] L. Kaelbling, M. Littman, and A. Cassandra, “Planning and Acting in Partially Observable Stochastic Domains,” *Artificial Intelligence*, vol. 101, no. 1-2, pp. 99–134, 1998.
- [17] G. Costante, J. Delmerico, M. Werlberger, and P. Valigi, “Exploiting Photometric Information for Planning under Uncertainty,” in *Robotics Research*. Springer, 2017, pp. 107–124.
- [18] A. Bry and N. Roy, “Rapidly-exploring random belief trees for motion planning under uncertainty,” in *IEEE International Conference on Robotics and Automation*. Shanghai: IEEE, 2011, pp. 723–730.
- [19] C. Richter, A. Bry, and N. Roy, “Polynomial Trajectory Planning for Aggressive Quadrotor Flight in Dense Indoor Environments,” in *International Symposium of Robotics Research*. Singapore: Springer, 2013.
- [20] F. Bourgault, A. A. Makarenko, S. B. Williams, B. Grocholsky, and H. F. Durrant-Whyte, “Information Based Adaptive Robotic Exploration,” in *IEEE/RSJ International Conference on Intelligent Robots and Systems*. Lauseanne: IEEE, 2002, pp. 540–545.
- [21] N. Hansen, “The CMA evolution strategy: A comparing review,” *Studies in Fuzziness and Soft Computing*, vol. 192, no. 2006, pp. 75–102, 2006.
- [22] L. Golshani and E. Pasha, “Rényi entropy rate for Gaussian processes,” *Information Sciences*, vol. 180, no. 8, pp. 1486–1491, 2010.
- [23] J. Solà, “Course on SLAM,” Barcelona, 2017.
- [24] J. Vallvé, J. Solà, and J. Andrade-Cetto, “Graph SLAM Sparsification With Populated Topologies Using Factor Descent Optimization,” *IEEE Robotics and Automation Letters*, vol. 3, no. 2, pp. 1322–1329, 2018.
- [25] M. Kaess and F. Dellaert, “Covariance recovery from a square root information matrix for data association,” *Robotics and Autonomous Systems*, vol. 57, no. 12, pp. 1198–1210, 2009.